Journal of Korean Institute of surface Engineering
Vol. 32, No. 3, Jun., 1999

TEXTURE AND RELATED PHENOMENA OF ELECTRODEPOSITS

D. N. Lee

Division of Materials Science and Engineering, and Research Center for Thin Film Fabrication and Crystal Growing of Advanced Materials, Seoul National University, Seoul 151-742, Korea,

Abstract

The texture of electrodeposits changes from the orientation that places the lowest energy crystal facets parallel to the substrate under a condition of low ion concentration adjacent to the deposit, to the orientation that places the higher energy crystal facets parallel to the substrate as the ion concentration adjacent to the deposit increases. The electrodeposits have peculiar surface morphologies and microstructures depending on their textures, which in turn may affect their mechanical properties even when they are obtained in a similar electrolysis condition. The electrodeposits undergo recrystallization, when annealed. The recrystallization texture may be different from the deposition texture. These phenomena have been discussed.

Key words : *electrodeposition, deposition textures, recrystallization txturs, microstructure, surface morphology, properties*

1. INTRODUCTION

Electrodeposits are known to have the preferred orientation or texture. The texture varies with electrolysis conditions, such as bath temperature, cathode current density, bath composition and agitation degree of electrolytes. Pangarov[1] suggested that the texture of fcc deposits changed from <111> to <110> with increasing overpotential. Lee et al.[2-6] found the opposite trend in electrodeposits obtained from copper or nickel single ion containing baths.

The texture of electrodeposits is also related to their microstructure and surface morphology, which in turn may affect their mechanical and other properties. Electrodeposits often undergo recrystallization upon annealing. The texture of recrystallized deposits may differ from that of as-deposited state. Therefore, understanding of their texture evolution is very important.

This paper provides a brief review of the texture and related phenomena, mostly copper electrodeposits.

2. ELECTRODEPOSITION AND TEXTURE MEASUREMENT

When the deposit plane is oriented normal to

the electric field direction, its texture or preferred orientation is symmetrical to the field direction or its growth direction, and is defined by the crystal orientation of the growth direction.

In many cases the texture can be measured using a diffractometer. In this case, the orientation of the deposit is expressed in terms of texture coefficients or texture factors of reflection planes. The texture coefficient, TC, of the (hkl) plane is defined by

$$TC(hkl)=\frac{I(hkl)/I_o(hkl)}{(1/n)\Sigma[I(hkl)/I_o(hkl)]} \quad (1)$$

where I(hkl) and I_0(hkl) are the integrated intensities of (hkl) reflections measured for an experimental specimen and a standard powder sample, respectively, n is the total number of reflection planes and Σ means the summation. When the TCs of all reflection planes are unity, the distribution of crystal orientation is random. When the TC of any (hkl) plane is larger than unity, a preferred orientation or texture exists, in which grains are oriented with their (hkl) planes parallel to the surface. The larger the value of TC, the greater the degree of the preferred orientation.

The texture factor, TF, of the (hkl) plane is defined by

$$TF=\frac{I(hkl)/I_o(hkl)}{\Sigma[I(hkl)/I_o(hkl)]} \quad (2)$$

It follows from eqs. (1) and (2) that

$$TC=nTF \quad (3)$$

The summation of TCs of all the reflection planes is equal to n, whereas TFs sum up to unity. When the TF of any (hkl) plane is larger than the mean value of TFs, a preferred orientation or a texture exists in which grains are oriented with their (hkl) planes parallel to the surface. When the TFs of all reflection planes are the same, the distribution of crystal orientation is random. A more accurate orientation can be obtained from pole figures, from which inverse pole figures and orientation distribution functions can be calculated. For DC electrodeposition, the bath composition and temperature and the cathode current density are major deposition variables.

3. TEXTURE

The texture coefficients of the reflection planes of copper deposits obtained from baths A and B are given in Table 1. The data in Table 1 indicate that the texture of electrodeposit changes from <111> to <110> through <113> with increasing bath temperature and the effect of solution concentration on the texture does not seem to be striking within the experimental range. The data in Table 2 also show the same trend. It can be seen from the data in Table 3 that if other conditions are the same, the higher copper concentration in the bath tends to give rise to the <110> orientation in preferance to the <111> orientation (bath E, 26℃, 20A/dm^2 and bath H, 26℃, 20A/dm^2). The same temperature and current density effects on the texture are the same as in the copper sulfate baths.

An increase in the current density decreases the copper ion concentration adjacent to the cathode, because the depletion rate of copper

Table 1. Texture coefficients for copper deposits obtained from copper sulfate baths A and B[5]

Temp. ℃	C.D. A/dm²	Bath A 170g/l $CuSO_4 \cdot 5H_2O$, 50g/l H_2SO_4				Bath B 240g/l $CuSO_4 \cdot 5H_2O$, 80g/l H_2SO_4			
		111	100	110	311	111	100	100	311
65	16	0.04	0.06	3.53	0.37	0.01	0.04	3.75	0.2
	20	0.14	0.16	3.28	0.49	0.03	0.28	3.52	0.17
60	14	0.08	0.2	3.12	0.56				
	16					0.03	0.04	3.58	0.35
	20	0.14	0	3.70	0.25	0.07	0.2	3.44	0.32
55	14	0.22	0.09	3.15	0.53				
	16					0.06	0.09	2.91	0.92
	20	0.14	0	3.75	0.14	0.12	0.66	2.65	0.58
50	10					0.03	0.24	3.28	0.47
	14	0.04	0.01	3.67	0.26				
	18					0.19	0.06	2.14	1.6
	20	0.14	0.06	3.2	0.62				
40	8	0.31	0.40	2.32	0.75	0.03	0.27	2.74	0.99
	12					0.22	0.47	2.03	1.26
	14	0.48	0.49	1.85	1.26				
	18	0.49	0.60	1.73	1.16	0.35	0.45	1.75	1.45
35	2					0.19	0.22	2.61	1.04
	10	0.99	0.25	2.2	0.55				
	14	1.71	0.57	0.51	1.5	0.14	0.98	1.89	0.99
	20	2.74	0.17	0	1.06	0.28	0.84	1.58	1.41
30	10	1.32	0.45	0.5	1.72				
	14					1	0.91	0.84	1.27
	18	1.4	0.31	0.11	2.21	1.21	0.83	0.4	1.56
	20	1.85	0.35	0	1.8	1.30	0.27	0.35	2.14
25	6	0.96	1.02	0	2				
	8					1.23	1.64	0.39	0.73
	10					1.37	0.78	0.33	1.52
	12	1.42	0.2	0	2.36				
	18	2.28	0.5	0	1.21	1.63	0.54	0.32	1.51
	20	2.51	0.2	0	1.3	2.08	0.32	0.23	1.27

Table 2. Texture fractions for copper deposits obtained from copper sulfate baths C and D[7]

Bath	Composition	Temp. ℃	Current Density A/dm²	TF		
				(111)	(100)	(110)
C	250g/l $CuSO_4 \cdot 5H_2O$ 70g/l H_2SO_4	30	0.5	0.14	0.86	0.0
D	280g/l $CuSO_4 \cdot 5H_2O$ 80g/l H_2SO_4	30	1-6	0.0	0.0	1.0
			8	1.0	0.0	0.0
		40	3-10	0.0	0.0	1.0
			12	1.0	0.0	0.0
		50	5-14	0.0	0.0	1.0
			16	1.0	0.0	0.0

Table 3. Texture fractions for copper deposits obtained from copper sulfate baths C and D[7]

Bath	Composition	Temp. ℃	Current Density A/dm²	TF			
				(111)	(100)	(110)	(311)
E	448g/l $Cu(BF_4)_2$	*20	30	0.21	0.14	0.39	0.26
	30g/l HBF_4	*40	30	0.01	0.01	0.97	0.01
	30g/l H_3BO_4	26	20	0.02	0.03	0.83	0.11
			30	0.05	0.24	0	0.71
			40	1	0	0	0
F	373g/l $Cu(BF_4)_2$	26	20	0.09	0.07	0.68	0.22
	25g/l HBF_4						
	25g/l H_3BO_4						
G	298g/l $Cu(BF_4)_2$	26	20	0.18	0.14	0.52	0.16
	20g/l HBF_4						
	20g/l H_3BO_4						
H	224g/l $Cu(BF_4)_2$	26	10	0.07	0.13	0.73	0.06
	15g/l HBF_4		20	1.0	0.0	0.0	0.0
	15g/l H_3BO_4		30	1.0	0.0	0.0	0.0

* These baths were agitated

ion due to reduction at cathode is higher than the diffusion rate of copper ion to the cathode. Increases in the bath temperature and agitation raise the diffusion rate of ions, and in turn increase the ion concentration adjacent to the cathode. Summarizing, the copper ion concentration adjacent to the cathode increases with increasing bath temperature, agitation, and copper ion concentration and decreasing current density. This is schematically shown in Fig. 1.

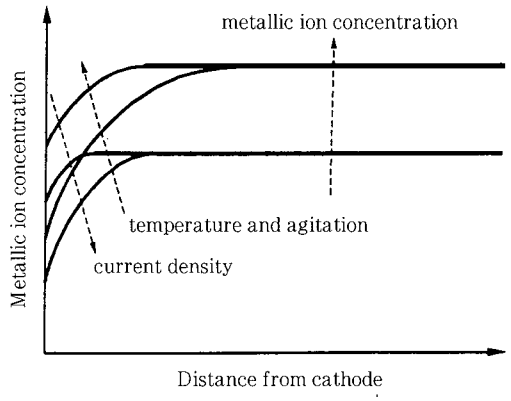

Fig. 1 Schematic figure showing effects of metallic ion concentration, temperature, agitation, and current density on metallic ion concentration gradient. Arrows indicate increasing directions.

The texture change depending on the electrolysis conditions can be stated as follows : As the metallic ion concentration adjacent to the cathode increases, the texture changes from the <111> orientation to the <110> orientation through the <311> orientation and vice versa. Noting that the lattice surface energy increases in the order {111}, {311} and {110} in the fcc as shown in Fig. 2, we reach the conclusion that the texture of electrodeposits changes from the orientation that places the lowest energy crystal facets parallel to the substrate under a condition of low ion concentration adjacent to the deposit, to the orientation that places the higher energy crystal facets parallel to the substrate as the ion concentration adjacent to the deposit increases. This was first noticed by Lee and Chang[2]. Later this has been shown to hold in electrodeposition of chromium[9], nickel[3,4,12] as

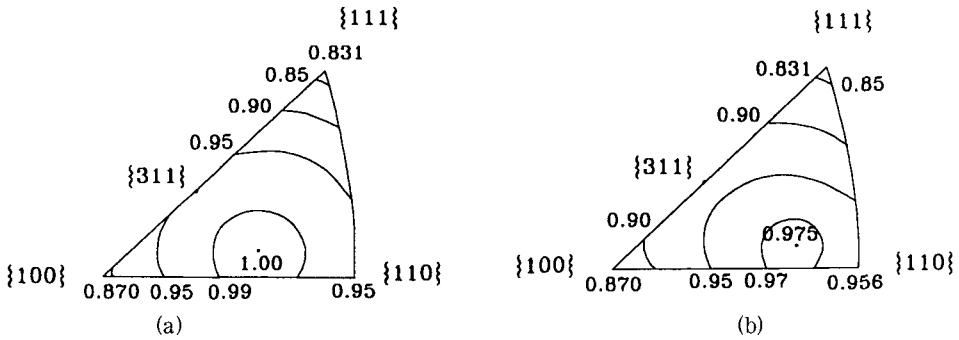

Fig. 2 (a) Measured and (b) calculated relative lattice surface energies of fcc metals [8].

well as copper.[5-7]

Fig. 3. shows a two-dimensional model of two adjacent crystals. The surface energy of a crystal facet parallel to plane CD of grain A is higher than that of grain B, that is, crystal A has a higher ledge density than crystal B ($\alpha > \beta$). Planes parallel to plane CE must be the most closely packed planes which have the minimum surface energy. Arrows indicate impinging ions. Squares attached to the surface of the crystal indicate newly reduced atoms. Atoms are not always reduced directly on to ledges. Atoms reduced on flat surfaces (M in Fig. 3a) are in a less stable state than atoms at ledges because they are less bonded than atoms at ledges. Therefore, they are liable to diffuse to ledges.

When the ion concentration adjacent to the deposit is high, crystal B is expected to have more atoms reduced between the ledges than crystal A, because the average diffusion distances on A is shorter than on B. Therefore, the configuration on crystal A is more favorable than that on crystal B, resulting in crystal A being in better position to grow than crystal B. In this case the deposit will assume the orientation of crystal A which has a higher surface energy plane normal to the direction of deposit growth. When the ion concentration adjacent to the deposit is low, the free moving distance of ions becomes long and ions have a better chance of reaching the ledges. The situation is shown in Fig. 3b. In this case, the surface area to be covered by reduced atoms is larger for

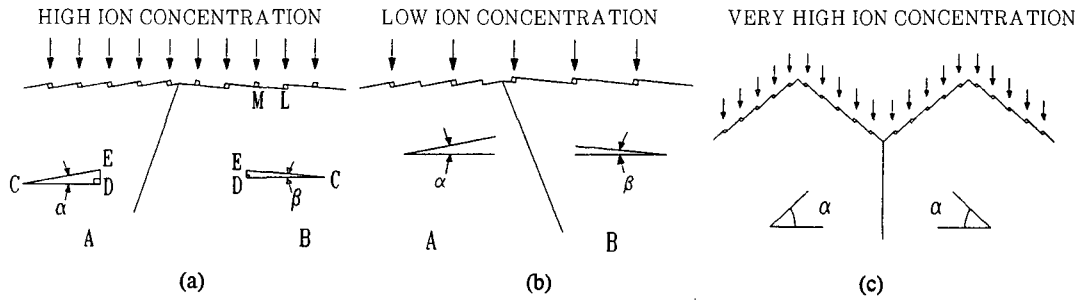

Fig. 3 Two-dimensional model explaining development of texture of electrodeposit.

crystal A than for crystal B, because the angle α is larger the than angle β. Therefore crystal B is in better position to grow than crystal A. In this case the deposit will assume the orientation of crystal B.

This selective growth model is based on the assumption that the crystal growth front is flat, the direction of impinging ions is normal to the deposit, the surface diffusion rate is high enough for reduced atoms to adjust themselves to stable position, and the relative lattice surface energies are not influenced by atmosphere covering the deposit. For copper plating, the above assumptions do not seem to be unreasonable.

If the ion concentration is too high for the ledges on flat deposit surface to accept, the deposit surface roughens to increase the ledge density (Fig. 3c). This is compatible with fact that rough surfaces are often observed in deposits with the <110> orientation. If impurity elements like carbon are codeposited as in cyanide bath I, the crystal growth is hindered by the impurity elements and the deposit tends to have very fine grains with the random orientation (Table 4).

If "ions" and "reduced" in this section are replaced by "atoms or ions" and "condensed or reduced", respectively, the model is applicable to vapor deposits[10,11].

4. MICROSTRUCTURE OF CROSS SECTION

The microstructure of the cross sections of electrodeposits are closely correlated with their preferred orientations[2-7,9,12]. The copper electrodeposits with the <100> texture shows a less-well-developed columnar structure with traces of twinning boundaries at about 30° to 40° with the growth direction (Fig. 4a). The microstructure of a deposit with the <110> texture is characterized by a fine field-oriented texture type structure that seems to be somewhat related to field-oriented twin boundaries (Fig. 4b). A deposit with the <111> texture has a lamellar twin structure in field oriented columns, as shown in Fig. 4c. These results can be explained, based on the fact that grains tend to grow along the electric field direction and {111} twin boundaries characterized by relatively straight lines, along with grain boundaries, constitute the microstructures.

Fig. 5 shows the orientation relation between the deposit orientation and the {111} planes. For clarity, not all the {111} planes are shown

Table 4. Texture fractions for copper deposits obtained from copper cyanide bath

Bath	Composition	Temp. ℃	Current Density A/dm	TF			
				(111)	(100)	(110)	(311)
I	89.5g/l CuCN	*40	0.25	0.39	0.15	0.19	0.27
	65g/l KCN			(0.53)	(0.31)		(0.16)
	40g/l $NaOH_4$	60	1.0	0.53	0.12	0.02	0.33
					(1.0)		

* TFs in parentheses indicate the values recrystallized specimens.

in the figures. Fig. 5a shows that traces of the {111} twin boundaries are at about 30° to 40° with a <100> growth direction (the [001] direction in Fig. 5a), in agreement with the experimental result in the deposit with the<100> texture. Fig. 5b shows that the {111} twin boundaries are at 90℃ with the {110} planes in the deposit with the <110> texture. It can be seen that the fine boundaries in the field direction in Fig. 4b consist of grain boundaries and twin boundaries. The lamellar twin structure in the deposit with the <111> texture in Fig. 4c is self-explanatory because a <111> direction is parallel to the field direction (Fig. 5c).

5. SURFACE MORPHOLOGY

Fig. 6a and b show the surface morphology of the copper deposit with the <100> texture, which is characterized by flat square facets. This reflects the fact that free surfaces of electrodeposited copper grains tend to be the {100} planes, as shown in Fig. 6c. The truncated edges of the square in the figure are thought to originate from the {110} planes.

Fig. 7a and b show the surface morphology of the copper deposit with the <111> texture. A magnified asperity is shown in Fig. 7b. There are two possibilities that the asperity assumes

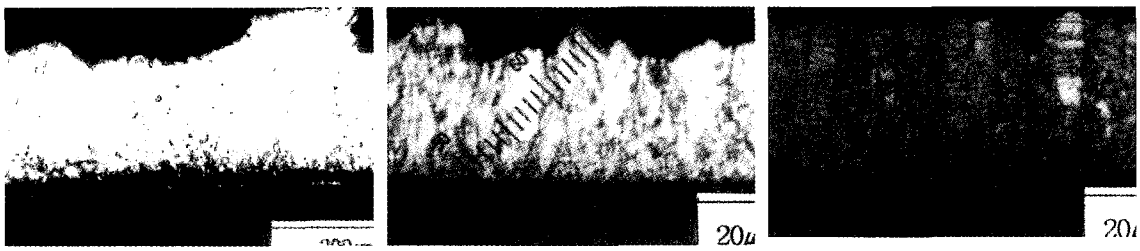

(a) (b) (c)

Fig. 4 Microstructures of copper electro-deposits, having (a) <100>, (b) <110> and (c) <111> textures, respectively.[6]

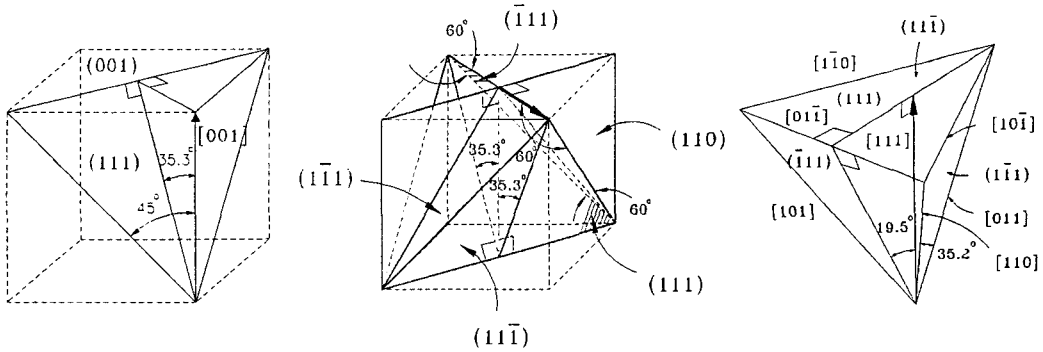

(a) (b) (c)

Fig. 5 Illustration of orientation of {111} planes in (a) <100>, (b) <110> and (c) <111> textures. Arrows indicate direction of growth.

the trigonal pyramidal shape. One is that the asperity is composed of three equivalent {111} planes as shown in Fig. 5c. Another is that it is composed of three equivalent {100} planes, as shown in Fig. 7c. If it is admitted that free surface tend to be the {100} planes, as in Fig. 6, a model of the asperity may be as shown in Fig. 7c.

Fig. 8 shows the surface morphologies of copper deposits with the <110>texture, character-

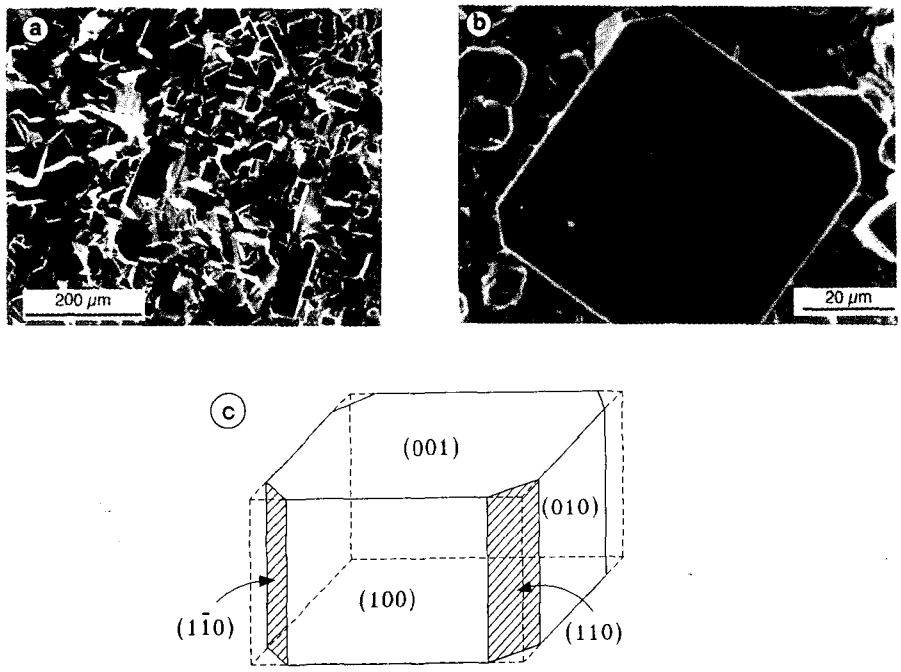

Fig. 6 Surface morphology of copper deposit having <100> texture. Fig.(c) shows that flat facets in (a) and (b) are {100} planes

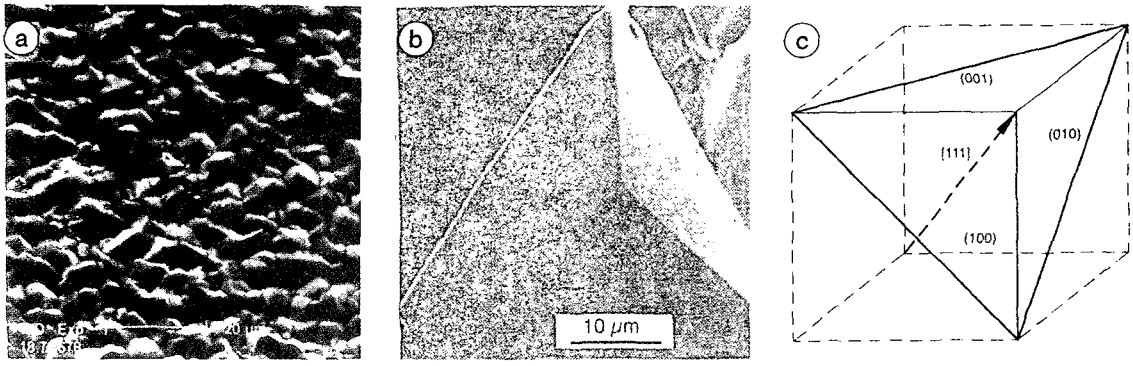

Fig. 7 Surface morphology of copper deposit having <111> texture. Fig.(c) shows that surfaces of asperities are {100} planes.

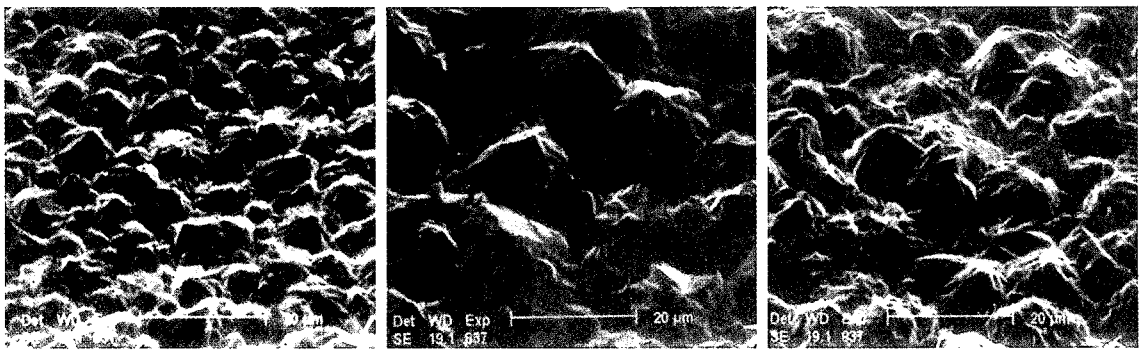

(a) (b) (c)

Fig. 8 Surface morphology of copper deposits with <110> texture obtained from bath D: (a) 30℃, 6A/dm²; (b) 30℃, 1A/dm²; (c) 50℃, 5A/dm².[6]

ized by asperities with ridges and valleys. One asperity consists of many twins growing outward, as shown in Fig. 9. The size of asperities decreases with increasing current density and decreasing temperature, as in the case of grain size.

6. MECHANICAL PROPERTIES

Fig. 10 shows the tensile strengths and elongations of 35㎛ thick copper foils obtained from baths A and B. The tensile strength decreases

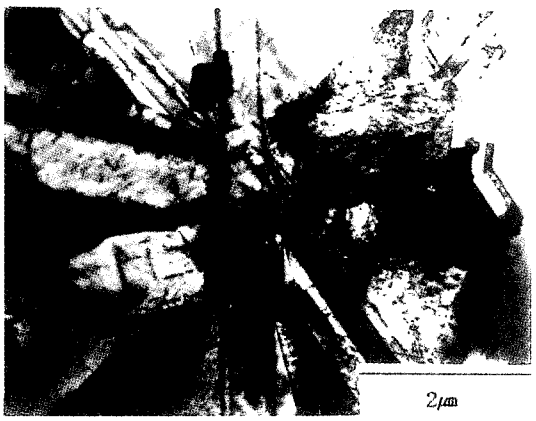

Fig. 9 TEM showing twins growing outward in deposit with <110> texture.[6]

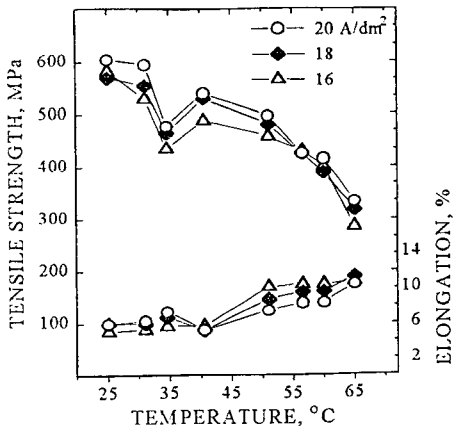

(a)

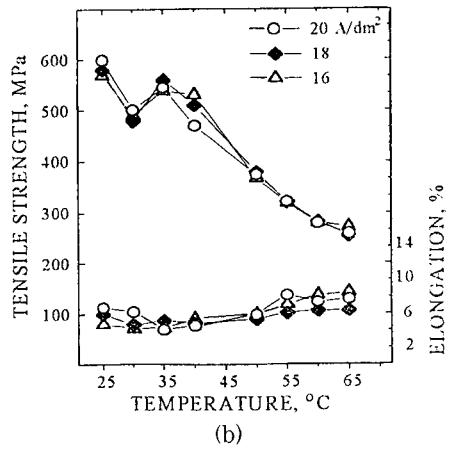

(b)

Fig. 10 Tensile strengths and elongations of 35㎛ thick copper foils obtained from baths A and B.[5]

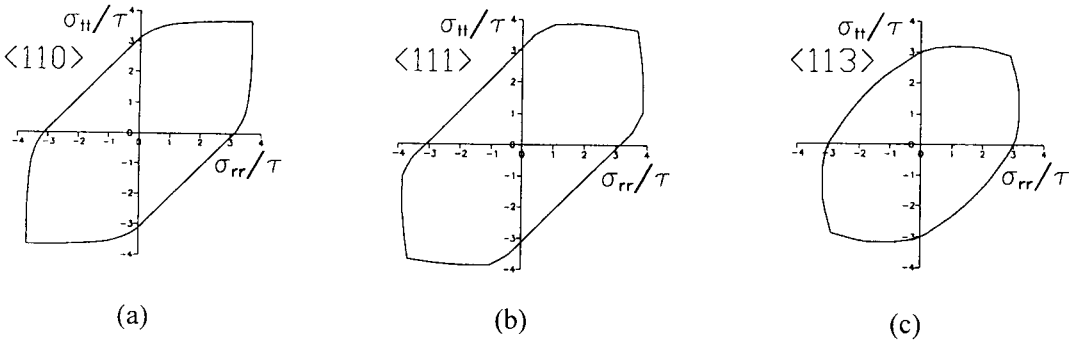

(a) (b) (c)

Fig. 11 Calculated yield loci for fcc sheets with (a) <110>, (b)<111> and(c) <113> textures.[13]

and elongation increases with increasing bath temperature. The results are expected, because, in general, the grain size increases and the dislocation density decreases with increasing bath temperature. However, the discontinuities observed in the tensile strengths are rather unusual. It can be seen from Table 1 that the specimens obtained from bath A below 35℃ and from bath B below 30℃ have the <111> + <311> texture, whereas those obtained above the temperatures have the <110> texture. Two factor may be considered to explain the discontinuity. One is the texture itself. Two different orientations may activate different slip systems and in turn give rise to different mechanical properties. Another is that the grain size may be influenced by the texture. Calculated yield loci in Fig. 11 indicate that the strength does not seem to be affected by the texture.

Since the deposits have fiber textures, the grain boundaries can be approximated by tilt boundaries. If electrolysis conditions are similar, the deposit whose grain bounday energy is smaller will have the smaller grain size than the deposit with the larger grain boundary energy. The average energy decreases in order of the <100>, <111> and <110> tilt boundaries as shown in Fig. 12[14]. Therefore, the <110> deposits will have finer grains than the <111> deposits, if they are obtained under similar electrolysis conditions. The discontinuities in Fig. 12 can be attributed to the grain size difference influenced by the texture. The coarse grain size was observed in the <100> nickel electrodeposits and the fine grain size in the <110> nickel electrodeposits[12]. This phenomenon may be similarly explained.

RECRYSTALLIZATION TEXTURE

The electrodeposits are well known to undergo recrystallization when annealed. Lee et al[6]. investigated recrystallization textures of copper electrodeposits having a simple texture like the <100>, <110> or <111> texture which were obtained from copper sulfate and copper fluoborate baths. Their results are summarized as follows: The <100>, <110> and <111> deposition textures change into the <100>, $<\sqrt{3}10>$ and <100>, respectively, on recrystallization.

These results were explained by Lee et al[6]. as

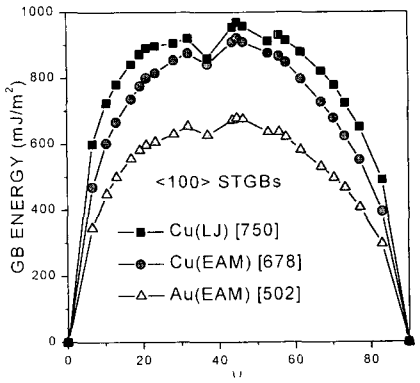

(a)

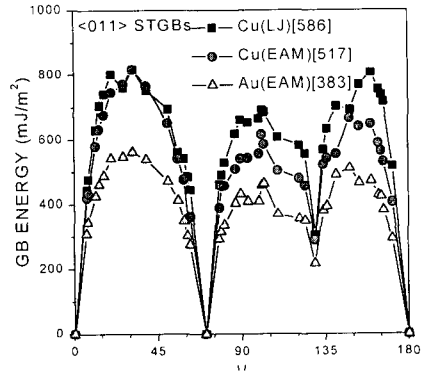

(b)

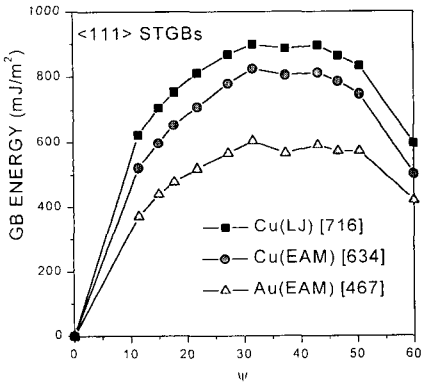

(c)

Fig. 12 Calculated Energy (in mJ/m²) for symmetrical tilt grain boundaries of fcc metals with interface planes perpendicular to (a) <l00>, (b) <011> and (c) <111> as function of tilt angle[14]. (LJ) and (EAM) indicate energies have been calculated using LJ and EAM potentials. Quantity in brackets indicates average tilt bounday energy.

follows: The driving force for recrystallization in the electrodeposits is attributed to the stored energy resulting from dislocations. Regardless of the kinds of dislocations, the Burgers vectors in fcc deposits are parallel to the <110> directions. A stable dislocation configuration, after an initial short-range interaction between neighboring dislocations during annealing, may be approximated by parallel edge dislocations, in which the direction of the absolute maximum internal stress is parallel to the Burgers vectors (Fig. 13)[15].

The recrystallized grains would orient themselves so that their minimum elastic modulus direction can be parallel to the absolute maximum internal stress direction of the original grains, whereby the strain energy release can be maximized, because recrystallization takes place in an approximately constant volume system. The minimum elastic modulus directions of copper are the <100> directions. Therefore, the <110> directions of the original copper grains, which are the Burgers vector directions of copper, tend to be oriented along the <100> directions

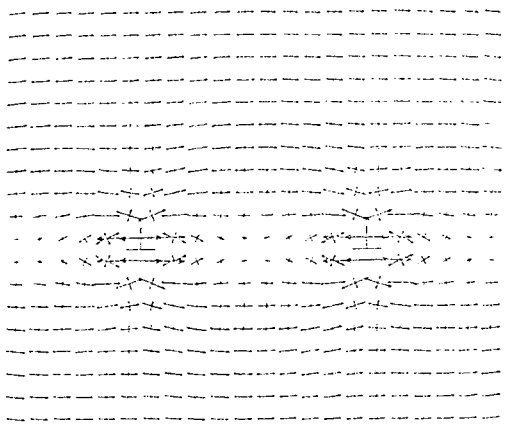

Fig. 13 Stress distribution around parallel edge dislocations[15].

of the recrystallized copper grains. There are six equivalent directions in the <110> directions, with opposite directions being taken as the same. Lee[16] suggested that the density of edge dislocations whose Burgers vectors are normal or nearly normal to the deposit growth direction would be higher than that of dislocations whose Burgers vectors are parallel or nearly parallel to the growth direction, because of the dislocation image force. This has been experimentally shown by Lee and Lee[17]. Therefore, the <110> directions normal or nearly normal to the thickness direction of the original deposit are the possible absolute maximum internal stress directions, which become the <100> directions after recrystallization.

For the deposit with the <100> texture, two of the six <110> directions are at right angles ; the remaining four are at an angle of 45℃ with the thickness direction, as shown in Fig. 14a. According to the above model, the former two <110> directions will change to the <100> directions after recrystallization. The recrystallized deposit would then have the <100> texture, as shown in Fig. 14b, in agreement with the experimental result.

For the <111> texture, three of the six <110> directions are at right angles with the thickness direction; the remaining three <110> directions are at an angle of 35.26℃ with the thickness direction, as shown in Fig. 5c. The former three <110> directions will be able to change to the <100> directions, after recrystallization, but angles between the <110> directions are 60° and the angle between the <100> directions is 90°. Correspondence between the <110> and <100> directions,

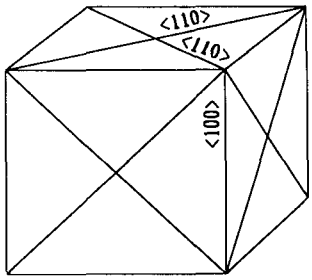

(a)

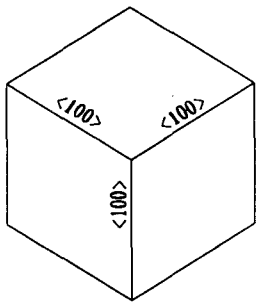

(b)

Fig. 14 Drawings explaining that <100> texture of copper deposit remains unchanged after recrystallization. (a) Before and (b) after recrystallization.

therefore, is impossible in a grain. Two of the <110> directions in neighboring grains, that are at right angles, may change to the <100> directions, however, to form nuclei having the <100> texture in grain boundaries, which grow at the expense of a high dislocation region, as shown in Fig. 15. Thus, the <111> texture will change into the <100> recrystallization texture, in agreement with the experimental result.

For the <110> texture, one <110> direction is normal to the <110> thickness direction; the remaining four <110> directions are at an angle of 60° with the <110> thickness direction, as shown in Fig. 15b. The first one of the <110> and the last four <110> directio-

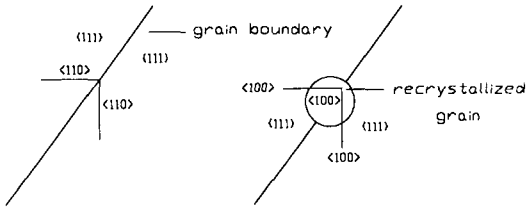

Fig. 15 Drawings explaining that <111> texture of deposit changes to <100> recrystallization texture.

ns are assumed to determine the recrystallization texture because the last four are closer to the planar direction than to the thickness direction. Recalling that the <110> directions change to <100> directions after recrystallization, it follows from Fig. 15b that the thickness direction of recrystallized grains should be at angles of 60° and 90° with the <100> directions at the same time. The thickness direction satisfying the condition will be $<\sqrt{3}10>$, which was measured by a pole figure device. The direction closest to this, that can be measured with a diffractometer, is the <210> direction, in agreement with the experimental result in Table 5.

Similar results have been obtained in silver electrodeposits[18].

CONCLUSIONS

1) The copper deposits with the <111> orientation have the lamellar cross sectional structure and trigonal pyramidal asperities on the surface.

2) The copper deposits with the <110> texture have the field oriented texture type structure, and the surface morphology of asperities with ridges and valleys.

3) The copper deposits with the <100> texture have a less well developed columnar structure with traces of twinning boundaries at about 30 to 40° with the growth direction and surface morphology having rectangular facets.

4) The copper deposits with the <111> texture tend to have the lower tensile strength than those with the <110> texture, when they are obtained in a similar electrolysis condition.

TAable 5. Texture fractions for copper deposits before and after annealing.

	Sample	TF						Approximate Texture
		(111)	(100)	(110)	(311)	(331)	(210)	
A	as-deposited	0.096	-	0.126	-	-	-	⟨100⟩
	recrystallized	0.062	-	-	-	0.131	-	⟨100⟩
B	as-deposited	-	-	0.92	0.06	-	⟨110⟩	
	recrystallized	-	-	-	0.07	0.93	⟨210⟩	
C	as-deposited	-	-	0.63	-	0.27	-	⟨210⟩
	recrystallized	-	-	-	0.20	-	0.80	⟨110⟩
D	as-deposited	1.0	-	-	-	-	-	⟨111⟩
	recrystallized	-	1.0	-	-	-	-	⟨100⟩

Samples A, C and D were obtained from copper sulfate baths, and sample B was obtained from copper fluobrate bath, The texture of samples with ⟨210⟩ was better represented by $\langle\sqrt{3}10\rangle$ from pole figure data.

5) The <100>, <111> and <110> textures of copper and silver electro-deposits change to the <100>, <100> and $<\sqrt{3}10>$ textures, respectively, when they are recrystallized.

ACKNOWLEDGEMENT

This study has been supported by KOSEF through RETCAM, Seoul National University.

REFERENCES

1. N. A. Pangarov (1962), Electrochimica Acta 7, 139.
2. D. N. Lee and Y. W. Chang (1974), J. Korean Inst. of Metals 12, 234.
3. D. N. Lee and G. C. Ye (1981), Plat. and Surf. Fin. 66 (11), 46.
4. G. C. Ye and D. N. Lee (1981), Plat. and Surf. Fin. 66 (4), 60.
5. D. N. Lee and Y. K. Kim (1985) in Proc. 2nd Asian Metal Finishing Forum, edited by H. Kanematsu (Tokyo Japan), p.130.
6. D. N. Lee, S. Kang and J. Yang (1995), Plat. and Surf. Fin. 82 (3), 76.
7. S. Kang, J.-S. Yang and D. N. Lee (1995), Plat. and Surf. Fin. 82 (10), 67.
8. B. E. Sundquist (1964), Acta Met. 12, 67.
9. J. R. Park and D. N. Lee (1979), J. Korean Inst. Metals 14, 359.
10. D. N. Lee (1989), J. Mater. Sci. 24, 4375.
11. D. N. Lee (1997), J. Korean Inst. Surf. Eng.29, 301
12. H. R. Lee and D. N. Lee (1985), in Proc. 4th Asian-Pacific Corrosion Control Conference, edited by S. Yoshizawa and K. Nii (Tokyo Japan), pp.955.
13. J.W.Kwon and D.N.Lee, unpublished result.
14. D.Wolf (1990), Acta Met. 38, pp.781
15. D. N. Lee (1995), Scripta Metall. Mater. 32, 1689.
16. D. N. Lee (1996), Metals and Materials 2, 121.
17. Y. S. Lee, and D. N. Lee : unpublished result.
18. H. S. Nam and D. N. Lee : unpublished result.